19th Australasian Fluid Mechanics Conference
Melbourne, Australia
8-11 December 2014

A Microfluidic Cross-Slot Device for Measurement of Erythrocyte Deformability

Y. Henon[1], G.J. Sheard[2] and A. Fouras[1]

[1] Laboratory for Dynamic Imaging, Department of Mechanical and Aerospace Engineering, Monash University, VIC 3800, Australia

[2] The Sheard Lab, Department of Mechanical and Aerospace Engineering, Monash University, VIC 3800, Australia

Abstract

Red blood cell (RBC) deformation is a dominant factor in the rheological properties of blood in vessels smaller than 300 micrometers. A reduction in cell deformability is associated with health conditions such as malaria and diabetes. The extensional flow within a microfluidic cross-slot microchannel has been proposed as a mechanism for measuring the deformation of cells. Three-dimensional simulations of red blood cell deformation in a microfluidic cross-slot channel are presented, suggesting the device has the capability of measuring both cell stiffness and viscosity.

Introduction

There is growing evidence that cell deformability is a useful indicator of cell health and may be useful in determining cell states or properties such as metastatic potential and degree of differentiation [8]. Diseases such as diabetes are known to increase erythrocyte stiffness, and the malaria parasite (*P. Falciparum*) progressively stiffens the erythrocyte it parasitizes [2,5]. The elasticity of red blood cells is a key factor in hemodynamics [13]. A number of methods, including atomic force microscopy, optical stretchers [18], and magnetic twisting cytometry [17] have been developed to study cell mechanics.

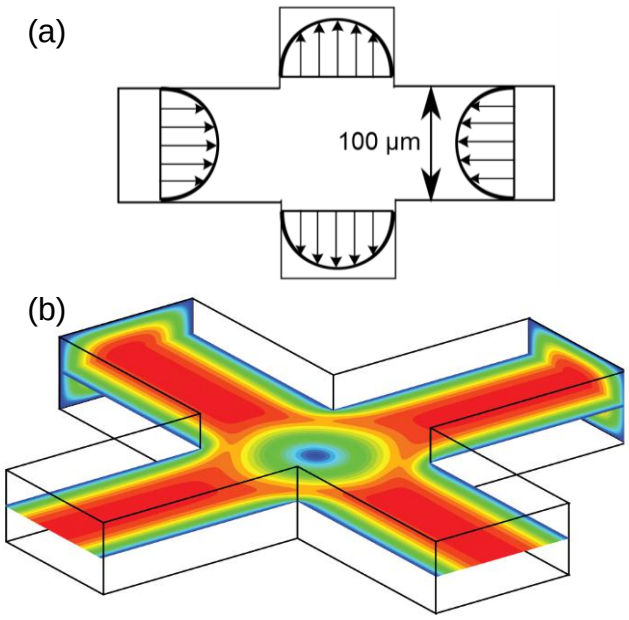

Figure 1. Geometry of the cross-slot device. (a) The cross-slot device consists of four arms, with two arms providing in-flow and two arms providing outflow, resulting in an extensional flow in the centre. (b) Contours of velocity magnitude, computed with an in-house computational fluid dynamics solver.

Microfluidic devices are being increasingly recognised as a useful way to measure cell properties with the potential for rapid and accurate measurement. They do not require delicate handling by specialised staff as is required by micropipettes and optical tweezers. Additionally, they allow these measurements in a physiological environment [3]. However, microfluidic devices alone only provide us with qualitative information about the observed phenomena and hence computational fluid dynamics can be critical in providing quantitative measurements.

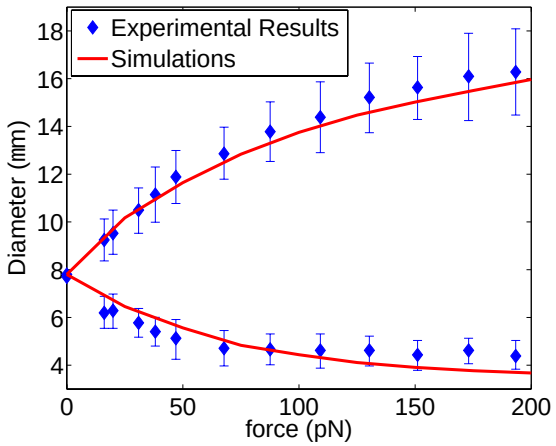

Figure 2. Simulated and experimental results of a red blood cell stretched with optical tweezers. Greater forces lead to greater stretching of the cell. There is generally a good agreement between the experiments and the simulations.

A microfluidic cross-slot channel featuring an extensional flow at the intersection between four channels, with two opposite channels providing inflow, and the two perpendicular channels providing outflow, was first introduced for the study of polymer extensional hysteresis [11] and has since been used to study polymer cells and beads [1], as well as for study of free vortex formation [10]. Due to the balance between inflow and outflow, an extensional flow is formed in the centre of the device, leading to extensional forces that are capable of stretching a sample such as a cell or a polymer. The sample being studied travels down one of the channel arms providing inflow, until it reaches the extensional region at the centre. At the device centre, the cell is trapped and becomes stationery. This cross-slot device has been shown to have the capacity to phenotype cells with a high throughput. Focussing cells into the device centre is one of the major challenges in designing a microfluidic cross-slot channel. The flow only approaches extensional flow in the centre of the device, as such cells that travel away from the device centre tend to deform less than cells that travel near the device centre. A number of approaches have been employed to focus cells, including the use of inertial forces [8] and employing viscoelastic

fluids [3]. Both methods are capable of increasing the fraction of cells travelling near the channel centre. An alternative approach, employing an active control system, has been proposed [4]. The simulations demonstrated the possibility for dynamic cell sorting to be achieved on a lab-on-a-chip device by integrating an active control system with a microfluidic cross-slot.

Results from simulations of erythrocytes trapped at the device centre are presented, with the intent of assessing the capability of such devices, allowing quantitative measurements to be made from experimental observations and providing guidance in the design of such devices. The magnitude of this deformation depends on the boundary conditions for the flow, the geometry of the device, the properties of the fluid in the device, and the properties of the cell.

Model description

Numerical technique

An immersed boundary method is employed, in which the Navier-Stokes equations for the fluid are solved on a fixed Eulerian grid while the forces arising from deformation of the cell are computed on a moving front [15]. A single set of equations are used for the entirety of the flow field, and allow variations in fluid density and viscosity [16].

The cell is modelled as an infinitely thin viscoelastic membrane, which surrounds the highly viscous haemoglobin contained within [9]. The technique employed has been shown to be able to simulate red blood cell deformation with accuracies close to experimental results [6]. The model has the capability to model cell membrane viscoelasticity, membrane bending resistance and membrane thermal fluctuations. It outperforms other models which rely on more simplified representations of the RBC [7]. Simulations of a RBC being stretched using optical stretcher are shown in figure 2. The figure shows the current numerical technique can accurately capture the cell deformation in a quantitative manner. The cell membrane model used within calculates forces on the cell membrane based on the potential energy of the system given as

$$V(\{\mathbf{x}_i\}) = V_{in-plane} + V_{bending} + V_{area} + V_{volume},$$

from which the forces can be derived as

$$\mathrm{f_i} = \frac{\partial V(\{\mathbf{x}_i\})}{\partial \mathbf{x}_\mathrm{i}}.$$

The in-plane forces are the contribution of the conservative elastic forces as well as the dissipative forces resulting from membrane viscosity. A nonlinear spring model is employed, the finitely extensible nonlinear elastic (FENE) spring, as it leads to better agreement with experimental results [6]. The area forces are included as erythrocytes are known to deform at constant surface area, resulting from the fact the membrane consists of a lipid bilayer that acts as a two dimensional fluid [12,14]. Volume forces are present as although the fluid is divergence-free, the interpolation of velocities performed in the immersed boundary method to move the cell mesh does not necessarily preserve the volume of the cell. Finally, erythrocytes have some resistance to bending, where the bending force resists membrane curvature and tries to return the cell to the initial undeformed state. An unstructured mesh is employed for the cell, which avoid issues relating to poles that result from structured meshing of surfaces with the topology of a sphere.

Device geometry and problem set-up

The device consists of four channel arms, of 100 micrometre width and 70 micrometre depth. Figure 1 gives a representation of the cross-slot device with velocity magnitudes shown as contours. These dimensions correspond realistically to microchannels currently being manufactured. Velocity Dirichlet boundary conditions for the channel inlets and outlets are imposed, where the velocity is given by the analytical solution for fully developed viscous flow through a duct with square cross-section. Zero-velocity no-slip boundary conditions are imposed at the wall. The use of a staggered variable arrangement obviates the need to define boundary conditions for pressure at the walls. The cell is located at or near the centre of the device, where the flow is resembles purely extensional flow. The cell is assumed to travel down the device centreline towards the centre of the device, where it deforms under the effect of the extensional flow.

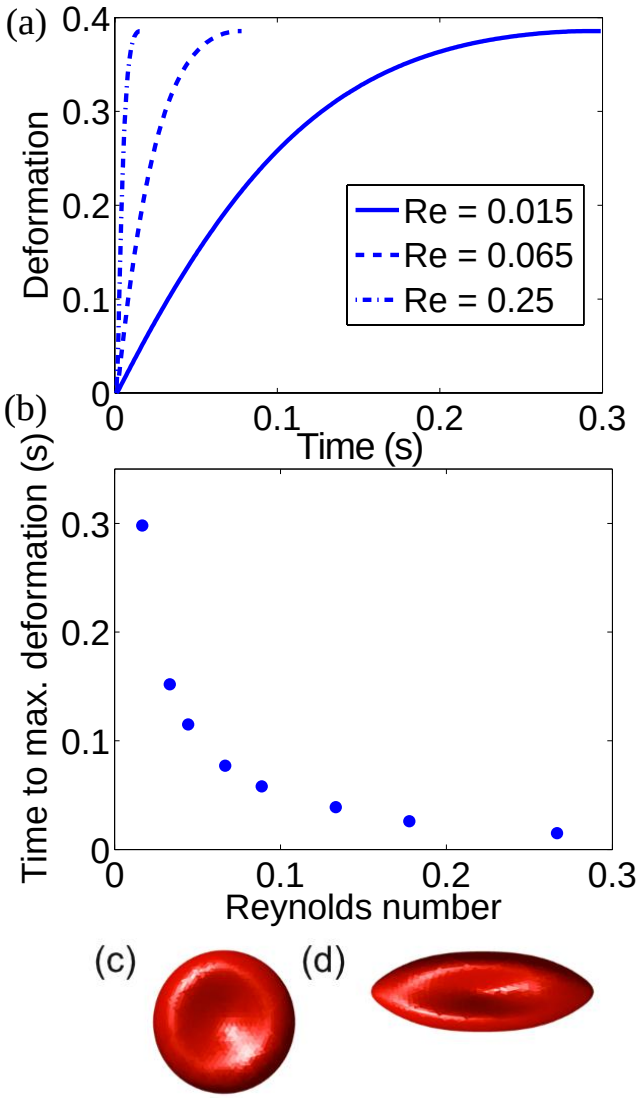

Figure 3. Time required for a red blood cell to reach its maximum deformation state in the cross-slot channel centre for different Reynolds number at a constant Capillary number Ca=0.5. (a) Time history of cell deformation for cells at Re = 0.015, Re = 0.065 and Re = 0.25, showing that the time required to reach maximum deformation decreases as Reynolds number increases. (b) Time required to reach maximum deformation for a red blood cell in a microfluidic cross-slot channel at a range of Reynolds numbers. (c) Shape of the undeformed red blood cell. (d) Shape of a red blood cell stretched in a microfluidic cross slot channel.

Throughout this study, the density and viscosity of the surrounding fluid are given as 1050 $\mathrm{kg \cdot m^3}$ and 1.0 $\mathrm{mPa \cdot s}$ respectively. The ratio of the viscosity of the cytoplasm to the surrounding fluid used is 5. The cell membrane elasticity is

$0.006\,\mathrm{dyn}\cdot\mathrm{cm}^{-1}$, unless indicated otherwise. The Reynolds number is defined for the device using the hydraulic length $D_h = \frac{2WH}{(W+H)}$, where W and H are the width and height of the device, respectively. It is also possible to define a cell Reynolds number, where the characteristic length is the radius of the cell. As the size of both the device and the cells are constant in this study, the choice of the device Reynolds number over the cell Reynolds number only changes the magnitude of the Reynolds numbers, but none of the trends.

Results

The Capillary number Ca is the dimensional number $Ca = \frac{\mu V}{E}$ used in quantifying the ratio of viscous forces to tension forces, in this case resulting from the red blood cell membrane, where μ is the fluid viscosity, V the fluid velocity and E the cell membrane stiffness. Figure 3a shows the behaviour of red blood cells in the cross-slot device for constant Ca = 0.5 and varying Reynolds numbers. Deformation is defined as $D = \frac{L-l}{L+l}$, where L is the length of the major axis and l the length of the minor axis. The maximum deformation of the cell is constant, but the time required for a cell to reach that deformation decreases as Reynolds number increases. For a given cell membrane elasticity, the maximum deformation depends on the magnitude of shear forces in the fluid. There are multiple contributors to the viscous behaviour observed, as the cell membrane has viscoelastic properties and the cell membrane surrounds a highly viscous fluid. Figure 3b shows that there is a highly significant decrease in the time required to reach maximum deformation over a moderate range of Reynolds numbers, from t_{max} = 0.016s at Re = 25 to t_{max} = 0.1 at Re = 0.015. This is significant in providing cross-slot devices with a way to assess cell viscosity, as the time required to reach the maximum deformation can be measured and related to the cytoplasm and cell membrane viscosity. Measurement of cell internal viscosity remains a challenge for techniques such as atomic force microscopy, and this represents a potentially important capability for microfluidic devices that is currently missing from other techniques.

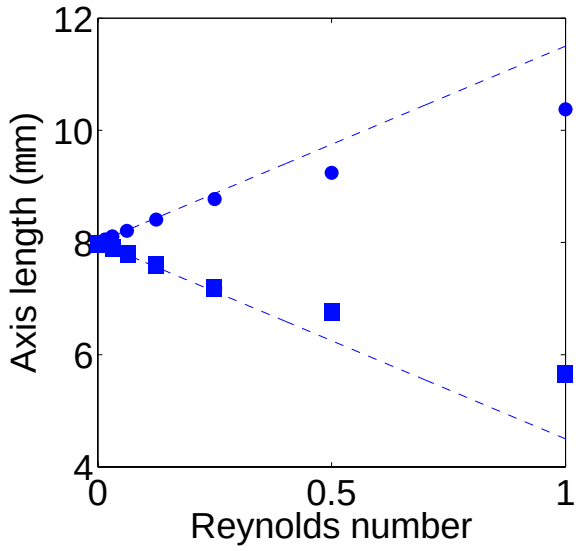

Figure 4. Length of major axis (circles) and minor axis (squares) as a function of Reynolds number. The lengths of the axes initially change linearly with Reynolds number. Beyond Re = 0.25, the rate of change decreases. Linear trend at small Reynolds numbers is shown with dotted lines.

Figure 3c shows the undeformed cell shape, while figure 3d shows a cell having reached its maximum deformation state in the cross-slot device. The cell has been stretched significantly by the action of the fluid forces, and the minor axis has decreased in length. There is a region of significant curvature at the tip of the cell, which is consistent with the knowledge that forces on the red blood cell membrane are dominated by elastic forces and resistance to area change, whereas the resistance to bending is small.

Cell deformation for a healthy red blood cell depends on the Reynolds number of the device. Figure 4 shows the length of the major and minor axis of a red blood cell stretched in the microfluidic device. The length of the axes initially increases linearly with Reynolds number at 0.25. Beyond this number, the increase in deformation with Reynolds number is sub-linear. This is expected from the nonlinear elastic model used in the simulations, where elastic forces increase in a superlinear way. The restriction on area change of the cell membrane also becomes more important when the cell is more stretched. At small deformations, the biconcave shape of the cell allows large stretching at constant area. However, when the cell has been stretched along its major axis, it becomes impossible to further stretch the cell while maintaining the surface area.

These results are consistent with the findings from optical stretchers (shown in figure 2), where the length of the axes increases quickly initially with applied force, and then show less change above a force of 100 pN. Unlike the optical stretcher, the relative increase in length of the cell major axis is equal to the relative decrease in length of the minor axis. In optical stretchers, both numerical simulations and experimental results indicate that the increase in length of the major axis is larger than the decrease in length of the minor axis. This is likely due to the fact that while optical stretchers apply forces in opposite direction at two tips of the cells, the cross-slot device applies forces at all points on the cell membrane. This results in the existence of forces compressing the cell along the minor axis. This change in cell shape can be seen in figures 3c and 3d.

Conclusion

Simulations of red blood cells in a microfluidic cross-slot channel have been presented, demonstrating the capability of such a device to measure the properties of red blood cells, including viscosity and elasticity, in a physiological environment. It was shown that the maximum deformation of cells depends on the membrane elasticity, and it is known that membranes elasticity strongly decreases under the effect of disease such as malaria. It was also shown that the viscous property of cells significantly affect the time required for cells to reach their maximum deformation state, suggesting that microfluidic devices are capable of measurement of cell viscosity, a capability lacking from many cell measurement techniques.

Acknowledgments

This research was supported by the Victoria Life Sciences Computation Initiative (VLSCI) grant VR00025, an initiative of the Victorian Government hosted by the University of Melbourne, Australia. G. J. Sheard is supported by the Australian Research Council through Discovery Grant DP120100153. A. Fouras is supported through NHMRC career development fellowship 1022721.

References

[1] Arratia P. E., Thomas C. C., Diorio J. & Gollub J. P., Elastic Instabilities of Polymer Solutions in Cross-Channel Flow, *Phys. Rev. Lett.*, **96**, 2006, 144502

[2] Babu N. & Singh M., Influence of Hyperglycemia on Aggregation, Deformability and Shape Parameters of Erythrocytes, *Clin. Hemorheol. Microcirc.*, **31**, 2004, 273-80.

[3] Cha S., Shin T., Lee S.S., Shim W., Lee G., Lee S. J., Kim Y., & Kim J.M., Cell stretching measurement utilizing viscoelastic particle focusing, *Anal. Chem.*, **84**, 2012, 10471–7.

[4] Curtis M. D., Sheard G. J. & Fouras A., Feedback Control System Simulator for the Control of Biological Cells in Microfluidic Cross Slots and Integrated Microfluidic Systems, *Lab Chip*, **11**, 2011, 2343-51.

[5] Dao, M., Lim C. T. & Suresh S., Mechanics of the Human Red Blood Cell Deformed by Optical Tweezers, *J. Mech. Phys. Solids*, **51**, 2003, 2259-80.

[6] Fedosov D. A., Caswell B., Suresh S. & Karniadakis G. E., Quantifying the biophysical characteristics of Plasmodium-falciparum-parasitized red blood cells in microcirculation, *Proc. Natl. Acad. Sci. U. S. A.*, **108**, 2011, 35–9.

[7] Fedosov D. A., Noguchi H., & Gompper G., Multiscale modeling of blood flow: from single cells to blood rheology, *Biomech. Model. Mechan.*, 2013.

[8] Gossett D., Tse H., Lee S. A., Ying Y., Lindgren A. G., Yang O. O., Rao J., Clark A. T. & Di Carlo D., Hydrodynamic stretching of single cells for large population mechanical phenotyping, *Proc. Natl. Acad. Sci. U. S. A.*, **109**, 2012, 7630-7635.

[9] Hochmuth R. M., Micropipette Aspiration of Living Cells, *J. Biomech.*, **33**, 2000, 15-22.

[10] Oliveira M. S. N., Pinho F. T., Alves M. A., Divergent streamlines and free vortices in Newtonian fluid flows in microfluidic flow focusing devices, *J. Fluid Mech.*, **711**, 2012, 171-191.

[11] Schroeder C. M., Babcock H. P., Shaqfeh E.S. & Chu S., Observation of Polymer Conformation Hysteresis in Extensional Flow, *Science*, **301**, 2003, 1515-9.

[12] Skalak R. & Branemark P.I., Deformation of Red Blood Cells in Capillaries, *Science*, **164**, 1969, 717-719.

[13] Sleep J., Wilson D., Simmons R. & Gratzer W., Elasticity of the Red Cell Membrane and Its Relation to Hemolytic Disorders: An Optical Tweezers Study, *Biophys. J.*, **77**, 1999, 3085-95.

[14] Svetina S., Kuzman D., Waugh R. E., Ziherl P. & Zeks B., The Cooperative Role of Membrane Skeleton and Bilayer in the Mechanical Behaviour of Red Blood Cells, *Bioelectrochemistry*, **62**, 2004, 107-13.

[15] Tryggvason G., Bunner B., Esmaeeli A., Juric D., Al-Rawahi N., Tauber W., Han J., Nas S. & Jan Y. J., A Front-Tracking Method for the Computations of Multiphase Flow, *J. Comp. Phys.*, **169**, 2001, 708-59.

[16] Unverdi S. O. & Tryggvason G., A Front-Tracking Method for Viscous, Incompressible, Multi-Fluid Flows, *J. Comp. Phys.*, **100**, 1992, 25-37.

[17] Van Vliet K. J., Bao G. & Suresh S., The Biomechanics Toolbox: Experimental Approaches for Living Cells and Biomolecules, *Acta Materialia*, **51**, 2003, 5881-905.

[18] Zhang H. & Liu K. K., Optical Tweezers for Single Cells, *J. R. Soc. Interface*, **5**, 2008, 671-90.